論文 / 著書情報
Article / Book Information

Title	Mangrove forest recovery a decade after Super Typhoon Haiyan
Authors	Hiroshi Takagi
Citation	Journal of Environmental Management, Vol. 395, ,
Pub. date	2025, 12
DOI	https://dx.doi.org/10.1016/j.jenvman.2025.127840
Creative Commons	Information is in the article.

Journal of Environmental Management 395 (2025) 127840

Contents lists available at ScienceDirect

Journal of Environmental Management

journal homepage: www.elsevier.com/locate/jenvman

Research article

Mangrove forest recovery a decade after Super Typhoon Haiyan

Hiroshi Takagi

School of Environment and Society, Institute of Science Tokyo, Japan

ARTICLE INFO

Keywords:
Mangrove reforestation
Typhoon Haiyan
Storm surge
Wind
NDVI

ABSTRACT

Many mangrove forests in the Philippines were severely damaged by Typhoon Haiyan in 2013, one of the strongest tropical cyclones in recent world history. This study focuses on a specific patch of mangrove forest in Cancabato Bay, located in Tacloban—the city most severely affected. To assess the extent of typhoon-induced impacts on the forest, the intensities of wind, waves, and storm surge during the typhoon were hindcasted using an advanced meteorological-hydrodynamic coupling model. It is estimated that the storm surge and high waves, reaching up to 4.7 m and 1.3 m respectively, destroyed the predominantly *Rhizophora apiculata* mangrove forest. Beyond the effects of storm surge and waves, strong winds of up to 41 m/s appear to have caused further damage, particularly to taller trees. Intensive community-based reforestation activities were carried out between 2015 and 2018 to restore the damaged coastline. An analysis of the Normalized Difference Vegetation Index (NDVI), derived from Landsat 8 OLI satellite imagery, reveals that the mangrove forest fringe increased by an impressive 80 % compared to pre-disaster levels, clearly demonstrating successful recovery following Typhoon Haiyan. In 2019, another strong typhoon, Phanfone, struck the same region, but the planted mangroves appeared to have withstood the storm with minimal damage. This study provides a concrete example that even when a mangrove forest is devastated by a powerful typhoon, it can recover in a relatively short time with effective afforestation efforts.

1. Introduction

South and Southeast Asia contain the largest mangrove forest coverage, accounting for 43.8 % of the global mangrove area (FAO, 2023) . Although these regions provide ideal tropical environments for mangroves, they are highly vulnerable to natural disasters, particularly tropical cyclones (TCs) and tsunamis. The three most fatal TC disasters in the 21st century—Cyclone Sidr in Bangladesh (2006), Cyclone Nargis in Myanmar (2008), and Typhoon Haiyan in the Philippines (2013)—all occurred in this region (Takagi and Heidarzadeh, 2023).

Past tropical cyclones have had significant impacts on forest ecosystems. Cyclone Sidr damaged 30 % of the Sundarbans in Bangladesh, the world's largest mangrove forest, resulting in severe ecological losses. It took approximately three years for the ecosystem to regenerate (Bhowmik and Cabral, 2013; Halder et al., 2021). Cyclone Nargis devastated 80 % of the mangroves in the Ayeyarwady Delta, and the mangrove recovery rate after four years was estimated to be only 61 % (Win et al., 2020; Aung et al., 2013). Typhoon Haiyan damaged 8,568 ha of mangroves in the Philippines—about 3.5 % of the country's total mangrove area—with approximately 870 ha severely damaged, 1,820 ha moderately damaged, and 5,900 ha slightly damaged (Long et al., 2016). Beyond Asia, Hurricane Dorian—one of the strongest Atlantic hurricanes—made landfall in the Bahamas in 2019. It caused widespread damage to mangrove and pine forests due to storm surges that extended up to 10 km inland. After six months, these areas showed minimal signs of recovery (Wilchcombe et al., 2021). In addition to the likely damage caused by storm surges, strong winds are also believed to have played a significant role in mangrove damage. For example, during Cyclone Nargis in Myanmar (2008), taller mangroves experienced more broken stem damage, indicating the influence of strong winds (Aung et al., 2013). Cyclone Mocha, which struck Rakhine State, Myanmar, in 2023, also caused widespread wind damage to coastal vegetation, and in some areas, pioneer species are believed to have rapidly proliferated in the damaged forests within weeks (Thwin et al., 2025).

Tsunamis also pose significant threats to mangroves. The 2004 Indian Ocean Tsunami inflicted devastating damage on mangrove forests in several countries, including Sri Lanka (Dahdouh-Guebas et al., 2005), India (Kathiresan and Rajendran, 2005), Thailand (Yanagisawa et al., 2009), and Indonesia (Onrizal and Mansor, 2016). Notably, coastal villages without mangrove protection experienced high casualties, whereas areas with intact mangrove belts fared better (Kathiresan and Rajendran, 2005; Barbier, 2006; Environmental Justice Foundation,

E-mail address: takagi.h.bd49@m.isct.ac.jp.

https://doi.org/10.1016/j.jenvman.2025.127840
Received 26 June 2025; Received in revised form 9 October 2025; Accepted 28 October 2025
Available online 31 October 2025

2006; Alongi, 2008). However, the disaster mitigation role of mangroves remains one of the most undervalued ecosystem services they provide (Barbier et al., 2008). One reason for this is the difficulty in verifying its effectiveness. The effectiveness of mangroves in reducing disaster impacts depends on several factors, including forest width, water depth, and tree maturity, making their protective value difficult to quantify (Teh et al., 2009; Takagi, 2018).

Among Asian countries, the Philippines ranks sixth in mangrove forest area, with 256,482 ha, following Indonesia (3,189,359 ha), Malaysia (709,730 ha), Myanmar (502,911 ha), Bangladesh (495,136 ha), and India (432,592 ha) (Spalding et al., 2010). Despite this ranking, mangrove cover in the Philippines has declined drastically—from approximately 400,000 ha in 1918 to around 100,000 ha by 1987—primarily due to timber extraction and the expansion of aquaculture (Santiago et al., 1990). National and local government involvement is essential in reversing this trend, especially considering that 95 % of the country's aquaculture industry has developed on former mangrove land (Santiago et al., 1990). Especially, the restoration of mangrove forests after a disaster cannot rely solely on natural regeneration; active human intervention is essential. Governments are not always considered the sole or primary custodians of forest resources. Increasingly, policies and programs are being developed that involve local people as partners in forest land management. Local people are, in fact, considered potential partners in mangrove reforestation. Their involvement is believed to foster local stewardship of newly planted forests and increase the success rate of reforestation (Walters, 2004).

In contrast to Indonesia and Malaysia, where the risk of tropical cyclones is minimal, mangrove management in the Philippines must consider the frequent occurrence of typhoons. Despite substantial financial investment, the long-term survival rate of mangrove plantations in the Philippines remains low (Primavera and Esteban, 2008). For example, average planting survival rates in Palawan and Luzon islands were reported to be as low as 11 % (Wodehouse and Rayment, 2019). Low survival rates are largely attributed to inappropriate species and site selection (e.g., mudflats below mean sea level). Additionally, some newly planted mangroves may have been damaged by typhoons shortly after planting (Primavera and Esteban, 2008). Alongi (2008) also emphasizes that young mangrove plantations often lack resilience to storm surges unless they are established with appropriate spacing, species diversity, and hydrological planning.

Against this backdrop, the present study focuses on a specific mangrove forest in Tacloban City, Philippines, to address two key objectives. First, it aims to quantify the physical impacts of Typhoon Haiyan on the mangrove forest by thoroughly assessing the contribution of storm surge, high waves, and strong winds, generated by one of the most powerful typhoons in history, to its destruction. Second, it examines whether community-led reforestation efforts contributed to the recovery of the mangrove ecosystem ten years after the disaster. Post-disaster reforestation efforts should be judged not by the number of propagules planted, but by the extent of forest growth observed several years later. By documenting both the destruction and rehabilitation of this particular forest, the study seeks to offer practical insights into the sustainable management of mangrove forests vulnerable to tropical cyclones.

2. Typhoon Haiyan: an overview of storm surge damage

On November 8, 2013, Typhoon Haiyan—locally known as Yolanda—struck the Philippines with devastating force. Haiyan made landfall on Leyte Island at peak intensity, with maximum sustained winds reaching 160 knots—the strongest ever recorded in the western North Pacific (Takagi et al., 2014). It ranks among the most powerful typhoons to make landfall globally (Lin et al., 2014; Schiermeier, 2013). Exceptionally strong winds generated a massive storm surge and high waves, causing widespread destruction across many islands along its path (Bricker et al., 2014; Takagi et al., 2014). The disaster claimed at least 6,245 lives (NDRRMC, as of March 6, 2014). Economic losses in infrastructure and agriculture were estimated at approximately USD 776 million, making it the costliest natural disaster in Philippine history (TIME, 2013). More than ten years have passed since the typhoon, yet rebuilding livelihoods—particularly for low-income communities—remains highly challenging. Long-term policy planning and sustained support are essential for ensuring post-relocation stability and enhancing community resilience (Iuchi, 2024).

Tacloban City and its surrounding areas on Leyte Island—the focus of this study—were particularly hard-hit by the storm surge. Several detailed investigations have been conducted in this region (Takagi et al., 2014, 2016; Bricker et al., 2014). In Tacloban, the storm surge began around 7:00 a.m. and lasted until approximately 8:30 a.m., reaching a peak height of nearly 6 m (Mikami et al., 2016; Takagi et al., 2016).

Fig. 1 shows recorded storm surge heights in Tacloban, based on data from surveys by Takagi et al. (2014), Tajima et al. (2014), and Mikami et al. (2016). The mangrove forest examined in this study is located in Paraiso, as indicated on the map. The storm surge in this area reached nearly 4 m, indicating that the mangrove forest likely sustained significant damage.

3. Methodology and data

3.1. Analysis of mangrove forest area before and after Haiyan

This study focuses on a small mangrove patch in Paraiso Village (Barangay 83-A) in Tacloban City, which was dominated by 25-year-old planted *Rhizophora apiculata*, naturally growing *Avicennia marina*, and *Nypa fruticans* located further inland (Carlos et al., 2015). This plantation likely represents a planned coastal rehabilitation effort from the early 1990s, consistent with government- and community-led mangrove planting programs. Fig. 2 compares the conditions before and after Typhoon Haiyan, clearly showing that the mangrove forest was severely damaged and that most of the houses behind the forest were also destroyed (Fig. 2b). It can be inferred that the storm surge flattened the mangrove forest and simultaneously surged up the creek, inundating the village. However, following reforestation efforts carried out primarily between 2015 and 2018, the mangrove area appears to have nearly fully recovered several years after Haiyan (Fig. 2g and h).

Particularly after the 2004 Indian Ocean Tsunami, geoinformatics techniques have been widely used to assess mangrove damage, significantly improving the efficiency of damage identification (Yanagisawa et al., 2010; Kamthonkiat et al., 2011). In this study, Landsat 8 OLI (Operational Land Imager) satellite images (30-m pixel resolution), launched shortly before Typhoon Haiyan, were used to quantitatively examine changes in the extent of Paraiso's coastal forest before and after the typhoon. As an alternative satellite image, for example, the USGS EROS Archive's Expedited Visible Infrared Imaging Radiometer Suite (eVIIRS) Vegetation Monitoring product offers direct NDVI values on an approximate 10-day cycle. Although valuable for immediate post-disaster response, its relatively coarse 250-m spatial resolution poses challenges for application to small mangrove forests such as Paraiso.

The Normalized Difference Vegetation Index (NDVI), a commonly used indicator for assessing vegetation greenness, including mangrove forests (Chen et al., 2017), was calculated using the following equation:

$$\text{NDVI} = \frac{NIR - R}{NIR + R} \quad (1)$$

Where NIR and R refer to the near-infrared and red spectral bands, respectively. NDVI is highly sensitive to the presence of photosynthetically active vegetation in the plant canopy (Tucker, 1979). Landsat 8 OLI is equipped with nine spectral bands, among which Band 4 corresponds to the Red band (0.64–0.67 μm) and Band 5 to the Near-Infrared band (0.85–0.88 μm). Higher NDVI values indicate greater vegetation

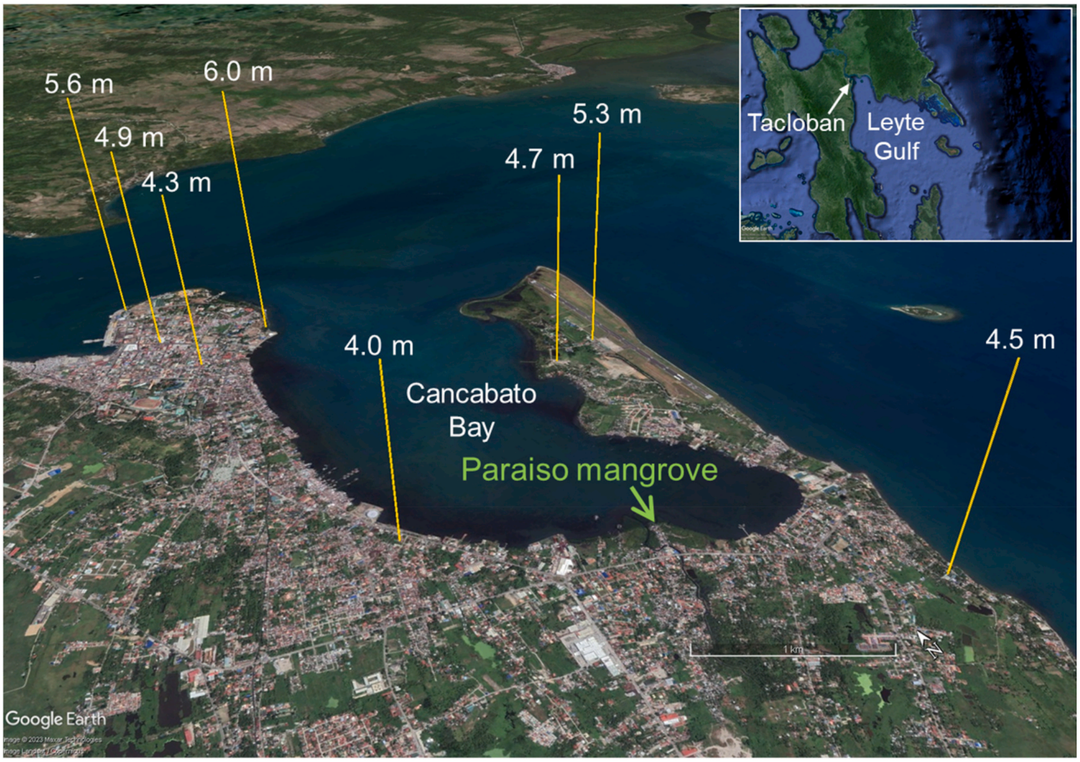

Fig. 1. Observed storm surge heights above sea level are plotted on a Google Earth satellite image (May 2013). The bar heights are based on storm surge observations reported by Takagi et al. (2014), Tajima et al. (2014), and Mikami et al. (2016). The Paraiso mangrove forest is located at the innermost part of Cancabato Bay.

greenness. A previous study of coastal areas in China found that NDVI values above 0.3 are indicative of mangrove forests (Chen et al., 2017).

However, the NDVI range may vary depending on the time and location. Yang et al., (2024) utilized NDVI derived from dense Landsat time series to monitor mangrove canopy condition, demonstrating that decreases reflect stress or degradation, while increases indicate recovery, and highlighting that NDVI values are not fixed but fluctuate seasonally. Ruan et al. (2022), who investigated global mangrove canopy density, reported that NDVI values varied significantly among regions, with the highest values observed in Southeast Asia, followed by South Asia and East Asia. Despite such uncertainties, for the sake of simplicity, this study used an NDVI threshold of 0.3.

3.2. Meteorological-hydrodynamic coupling model

A meteorological-hydrodynamic coupling model developed by Takagi et al. (2014) and Takagi and Takahashi (2022) was used to numerically analyze the wind waves and storm surge generated by Typhoon Haiyan (Fig. 3). The novelty of this method lies in its capability to simultaneously analyze the broad-scale meteorological field and the intense wind field near the typhoon center. For global weather reanalysis, the model employed the ECMWF Reanalysis v5 (ERA5), which provides hourly estimates of atmospheric, land, and oceanic climate variables from January 1940 to the present. Among the many available variables, only sea-surface wind and pressure were utilized, as they are particularly critical for the generation of storm surges and wind waves. This coupling model is also applied to Typhoon Phanfone, as described later; however, the analysis was confined to the Leyte Gulf rather than covering the entire Philippines.

The ERA5 model operates on a computational grid with a spatial resolution of 0.25° (approximately 27 km), which is clearly insufficient to resolve the fine-scale structure of a concentric low-pressure system. Therefore, in the present model, the typhoon's central region was replaced with an empirically derived parametric typhoon model (Schloemer, 1954; Myers, 1954). For this purpose, the typhoon's center location was determined using best-track data from the Japan Meteorological Agency (JMA). The model also incorporated super-gradient winds, which occur near the typhoon center and exceed the speed of gradient winds (Mitsuta et al., 1988).

For storm surge simulation, the Delft3D FLOW model (Deltares, 2011) was employed. Although this model supports both two- and three-dimensional simulations, the two-dimensional configuration—commonly used in nonlinear long-wave storm surge analysis (Takagi et al., 2020)—was selected for this study. The Alternating Direction Implicit (ADI) method was used for time integration, while the cyclic method was applied for spatial discretization of advection terms. Bathymetric data were sourced from the General Bathymetric Chart of the Oceans (GEBCO). For bottom friction, Manning's coefficient—commonly used in tsunami modeling—was set to 0.025 s $m^{-1/3}$ (Headquarters for Earthquake Research Promotion, 2017).

To simulate wind waves, the Simulating WAves Nearshore (SWAN) model (TU Delft, 2000) was used. SWAN is a third-generation wave model capable of simulating wind-generated irregular waves in coastal regions (Booij et al., 2000). In this study, the Komen model was selected for wave generation and dissipation due to wave breaking in deep water (Komen et al., 1984), and the Battjes and Janssen model was adopted for wave breaking in coastal regions (Battjes and Janssen, 1978). A two-way coupling analysis was performed between Delft3D FLOW and SWAN, enabling the exchange of water levels and velocities between the two models.

Focusing on the innermost waters of Leyte Gulf (San Pedro Bay), where Tacloban City is located, the computational domain was resolved using a 66-m spatial grid. To minimize computational cost, the outer boundary of this narrow region received input from a larger-scale simulation conducted by Takagi et al. (2014). The accuracy of this earlier model has been validated against observed storm surge data at various locations within Leyte Gulf. The accuracy of the storm surge level calculated by this model was also validated by Takagi et al. (2016)

Fig. 2. Condition of the mangrove forest in Paraiso: (a) before and (b)–(h) after Typhoon Haiyan (© Google Earth).

using observed water marks and eyewitness accounts at 14 locations in Tacloban City. The coefficient of determination ($R^2 = 0.574$) indicates that the model has relatively high reliability.

This comprehensive modeling framework enables the simulation of multiple variables, including wind speed, wind direction, water level rise, current velocity, wave height, and wave period at each grid point—allowing for a detailed assessment of the external forces that acted upon the mangrove forest during Typhoon Haiyan (Fig. 4).

3.3. Historical analysis of typhoon tracks around Leyte Island

Takagi and Esteban (2016) analyzed the unusual statistical characteristics of Typhoon Haiyan using best track data from the Joint Typhoon Warning Center (JTWC), covering the period from 1945 to 2013 and focusing specifically on tropical cyclones that made landfall in the Philippines. The approximate landfall point of each tropical cyclone (TC) was identified by detecting where the TC track intersects the

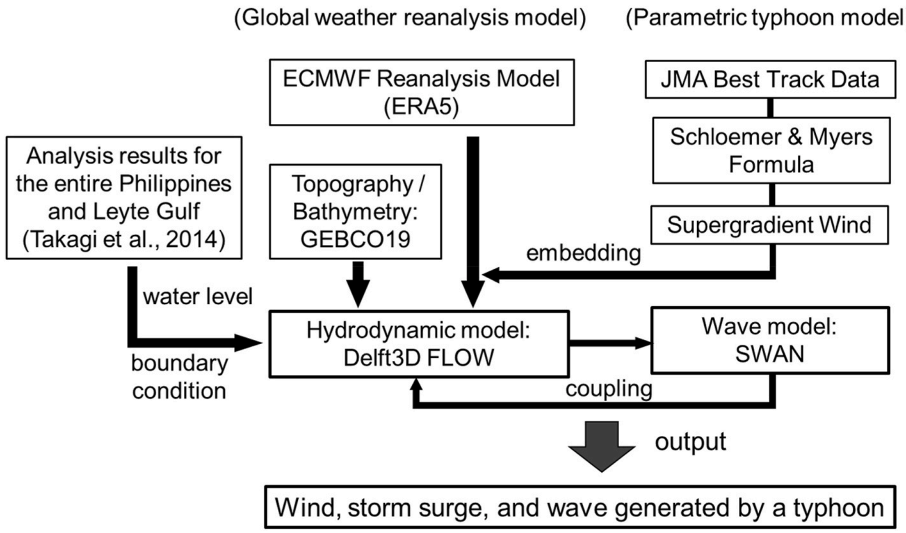

Fig. 3. Meteorological-hydrodynamic coupled model for estimating external forces.

coastline, using the Global Self-consistent, Hierarchical, High-resolution Shoreline Database (GSHHS) provided by the University of Hawaii and NOAA.

TC intensities at the time of landfall were estimated by interpolating the Best Track Data points recorded immediately before and after landfall. Among more than 400 recorded storms, Haiyan exhibited the highest wind speeds on record (165.8 knots)—approximately 16 % stronger than those of Typhoon Zeb (142.7 knots), the second most intense typhoon, which struck in 1998. The statistical return period for a typhoon of Haiyan's intensity was estimated at once every 200 years, compared to once every 19 years for Typhoon Zeb. Building upon their methodology, this study extends the analysis using the best track data up to 2022 and examines typhoons that approached Leyte Island in the period following Typhoon Haiyan. It should be noted that the JTWC classifies wind speed as a 1-min sustained wind. This measurement is typically higher than a 10-min sustained wind, a standard adopted by many agencies, such as the Japan Meteorological Agency (JMA), for the same storm.

4. Results

4.1. Forest cover before and after Typhoon Haiyan

Fig. 5 illustrates the changes in NDVI over a period of approximately 10 years, from August 2013 (just before the typhoon) to November 2023 (10 years after the typhoon). By identifying pixels with higher NDVI values (>0.3), the original mangrove area three months before Haiyan (Fig. 5a) was estimated to be roughly 2 ha (22 pixels). Three months after the typhoon (Fig. 5b), the NDVI in this area dropped below 0.2, indicating mangrove loss or dieback.

At 16 months and 3.6 years post-Haiyan (Fig. 5c and d), NDVI values increased in terrestrial areas but showed no significant recovery along the coast, suggesting that mangrove forests had not yet regenerated. This lack of recovery is also evident in Fig. 2c and d. The disappearance of mangrove vegetation appears to have contributed to the erosion of coastal sediments. Interestingly, however, 6.5 years after Haiyan (Fig. 5e), a marked increase in NDVI values is observed across a wide coastal area. This recovery is also visible in the rapid expansion of mangrove forests shown in Fig. 2g and h. By the 10th anniversary of the typhoon (Fig. 5f), the mangrove area had expanded to an estimated 3.6 ha (40 pixels).

The observed 80 % increase in mangrove area, exceeding its pre-Haiyan extent, can be attributed to reforestation efforts undertaken by the Paraiso community in collaboration with NGOs, government agencies, and international organizations. For example, between 2015 and 2018, approximately 30,000 mangrove seedlings were planted across 4 ha of land, with funding provided by the Japanese Ministry of Foreign Affairs (MOFA, 2022). The community had originally planted *Nypa fruticans*, a species with widely spreading leaves, but these were uprooted and washed away by Haiyan's storm surge, damaging nearby homes. Consequently, deep-rooted *Rhizophora* species, such as *Rhizophora mucronata* and *R. apiculata*, were selectively planted (Cho, 2017). These mangroves have since grown healthily, as reflected in the significant increase in NDVI values following the reforestation project.

4.2. Statistical significance of Haiyan and Phanfone

Typhoon tracks around Leyte Island in the Philippines were mapped using Joint Typhoon Warning Center (JTWC) Best Track Data from 1945 to 2022 (Fig. 6). Located along a common typhoon pathway, Leyte Island is struck by tropical cyclones almost annually. In the decade following 2013, aside from Typhoon Haiyan, Typhoon Phanfone (locally known as Ursula), which struck in December 2019, was particularly significant. It resulted in 28 fatalities and left at least 12 people missing (The Guardian, 2019).

The mangrove reforestation efforts in Paraiso were carried out specifically within three years between March 2015 and March 2018. Typhoon Haiyan and Typhoon Phanfone occurred before and after this period, respectively. As discussed in the previous section, the mangrove forest in Paraiso was severely damaged by Haiyan but has since undergone successful recovery through focused reforestation efforts. It is evident from Fig. 2 (g, h) and Fig. 5 (e, f) that Phanfone did not cause any significant damage to the regenerated mangroves.

This disparity is directly attributable to Haiyan, which was one of the strongest typhoons ever to affect the Philippines (an event with a 200-year return period), whereas Phanfone exhibited weaker momentum. The sheer scale of Haiyan, identified as a once-in-200-year typhoon in the Philippines, rendered the destruction of mangrove forests unavoidable. However, it is important to note that Phanfone was also by no means a weak storm. At landfall, it recorded a wind speed of 90 knots and a central pressure of 972 hPa. Typhoons of this magnitude are relatively common in the Philippines, typically occurring once every one to two years (Takagi and Esteban, 2016) (Fig. 7), whereas such intense tropical cyclones are regarded as very strong even in some other TC-prone countries.

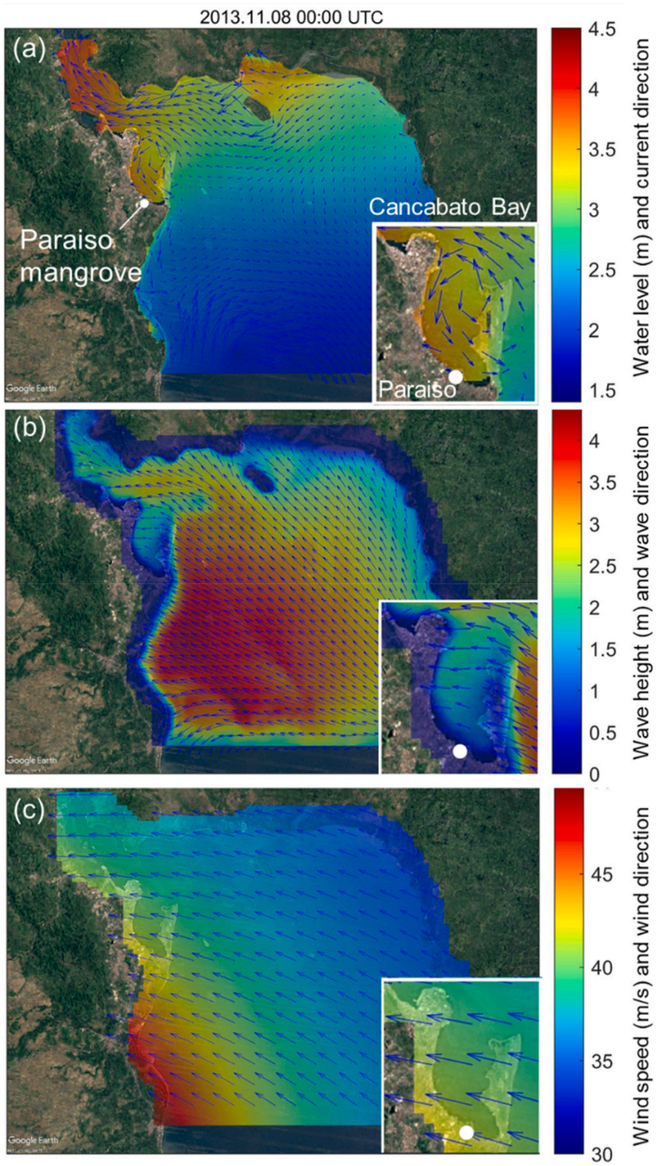

Fig. 4. Representative outputs generated by the meteorological-hydrodynamic coupled model. Case study for Typhoon Haiyan.

4.3. Estimated storm surge, waves, and winds: Haiyan vs. Phanfone

The meteorological-hydrodynamic coupled model was applied to hindcast the intensity of storm surge, waves, and wind, producing time history plots for two typhoons (Fig. 8a and b). The vertical axes of both figures are scaled identically to allow for an easy comparison of magnitudes between Haiyan and Phanfone. Given an initial water depth of approximately 1 m at this location in Cancabato Bay, the storm surge rise can be estimated by subtracting the initial depth from the maximum depth.

During Typhoon Haiyan, the maximum water depth reached 4.7 m, a figure consistent with measured heights of 4.0 m and 4.7 m at the closest observed points in Cancabato Bay (Fig. 1). Generated by strong winds up to 41 m/s, wind waves reached 1.3 m as they propagated on the surface of the storm surge, likely battering the canopy of mangroves, predominantly tall *Rhizophora apiculata* species. The water current during Haiyan was estimated at 0.45 m/s. Although this flow was generally not considered very fast, the combined impact of external forces was clearly strong enough to damage the entire mangrove forest in Paraiso.

In comparison to Haiyan, all external forces during Phanfone appear considerably smaller. The maximum wind speed during Phanfone was 20.7 m/s, approximately half that of Haiyan. Given that the generation of both wind waves and storm surge is essentially proportional to the square of wind speeds, the significantly weaker winds during Phanfone should have resulted in a lesser physical impact on the mangrove forest. In addition, the southeasterly wind at the time of Phanfone's landfall (Fig. 8d) helped push seawater from the end of the bay toward its entrance, thereby limiting the water level rise caused by the storm surge. In contrast, Haiyan's predominantly northerly wind direction (Fig. 8c), which blew toward the end of the bay, unfavorably generated storm surge in the uppermost part of the bay, where the mangrove forest is located. Therefore, the external forces generated by Haiyan should be acknowledged as the most unfavorable conditions regarding both their magnitude and direction.

5. Discussion on the key factors behind the success of reforestation

Since Typhoon Phanfone struck the area 2–4 years after planting, the mangroves were still in their juvenile stage. However, previous studies have shown that even relatively young mangroves can be resistant to typhoons. For example, a field study by Zhang et al. (2022) found that recently planted mangrove forests (2–6 years old) in Guangdong, China, withstood Typhoon Mangkhut in 2018. Similarly, Takagi (2023) investigated the survival of young planted mangroves in a calm bay environment. In that case, a strong typhoon (Typhoon Haishen) passed near Amami Island, Japan, just 16 months after *Kandelia obovata* had been planted. Despite being located on the seaward edge of the intertidal zone, most of the young mangroves survived without any visible damage. This is likely due to a suitable sheltering environment: although large waves over 10 m high were generated offshore, the mangrove forest was located in the innermost part of the bay, resulting in significant wave attenuation to less than 0.2 m.

The ability of mangroves to mitigate damage caused by tropical cyclones and tsunamis is considered one of the most undervalued ecosystem services provided by mangrove forests (Barbier et al., 2008). Therefore, extending beyond their ecological conservation implications, a heightened awareness among local populations regarding mangroves' role as natural buffers would be instrumental in galvanizing more proactive mangrove conservation initiatives. Established by the Paraiso community, the Paraiso Mangrove Eco-Learning Park exemplifies a nature-based solution for post-disaster recovery. It highlights the crucial integration of environmental education, nature conservation, and community empowerment to foster resilient coastal ecosystems (Fig. 9d). To serve as a disaster legacy, establishing a residents' mangrove education center in the affected areas is considered good practice.

Abayon (2023) also examines the socio-ecological dynamics of mangrove management in the aftermath of Typhoon Haiyan, highlighting the essential role of local communities, while also noting a lack of knowledge about mangrove species. In Tacloban, *Rhizophora apiculata* (tall-stilt mangrove) is the most common mangrove species, alongside *Sonneratia alba* (Cañete et al., 2018; Patindol and Casas, 2019). Informed knowledge of species-specific characteristics of mangroves is essential for local communities to implement sustainable practices that safeguard these critical coastal ecosystems. *Rhizophora* species, the predominant mangroves in Tacloban, have been shown to be more susceptible to mechanical damage than other tree species due to their prop roots, which are typically elevated above the substrate rather than embedded in it, making them more prone to breakage during typhoons (Asbridge et al., 2018). Tall mangroves are particularly vulnerable to strong winds (Halder et al., 2021), as confirmed in Fig. 9a. The mangroves that had grown sufficiently after planting also appear to be very tall (Fig. 9b), yet they survived Typhoon Phanfone. This difference in outcome may be partly attributed to the fact that wind speeds were significantly lower than during Haiyan (Fig. 8), and fortunately, Phanfone struck when the

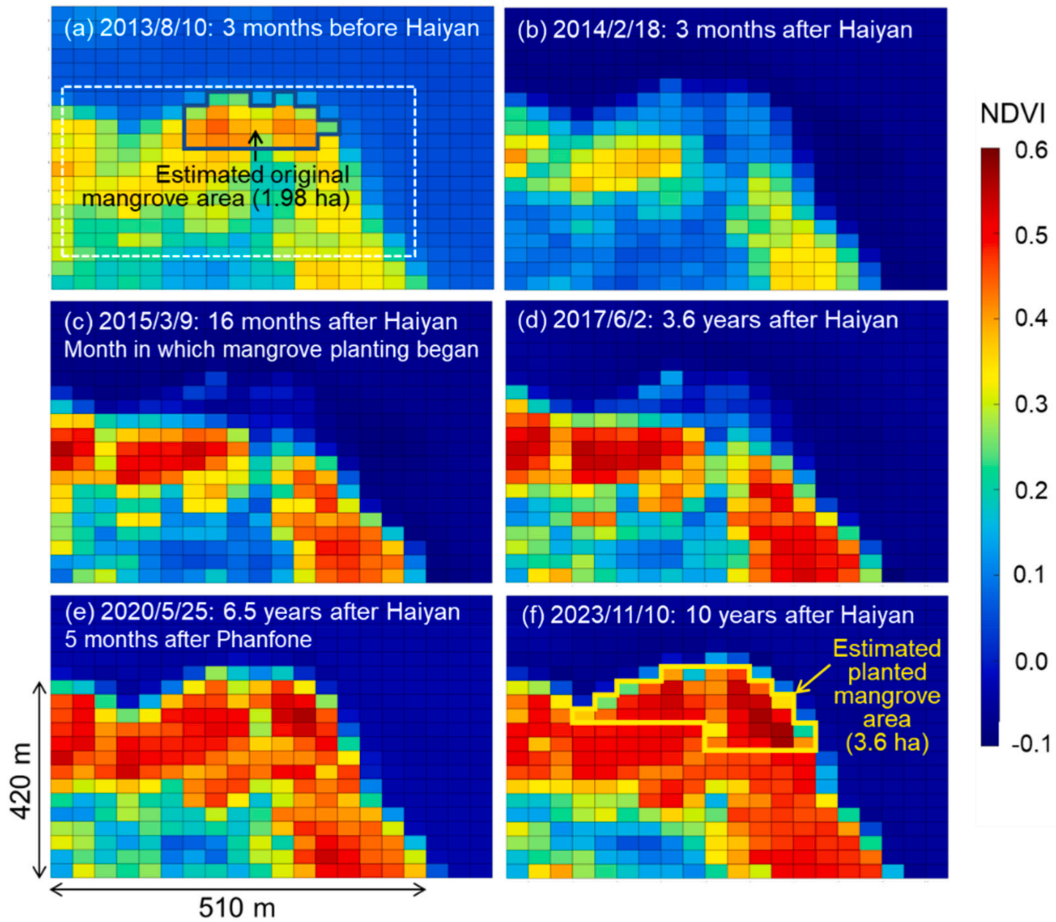

Fig. 5. A 10-year analysis of NDVI value changes around Paraiso, Tacloban City, encompassing the period before and after Typhoon Haiyan. The white dashed line shown in (a) corresponds to the area depicted in the satellite image in Fig. 2.

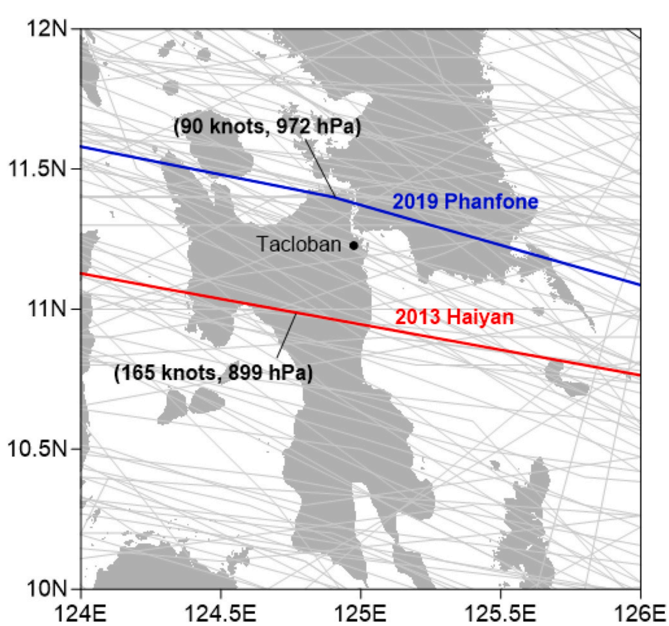

Fig. 6. Typhoons and tropical storms affecting Leyte Island (1945–2022).

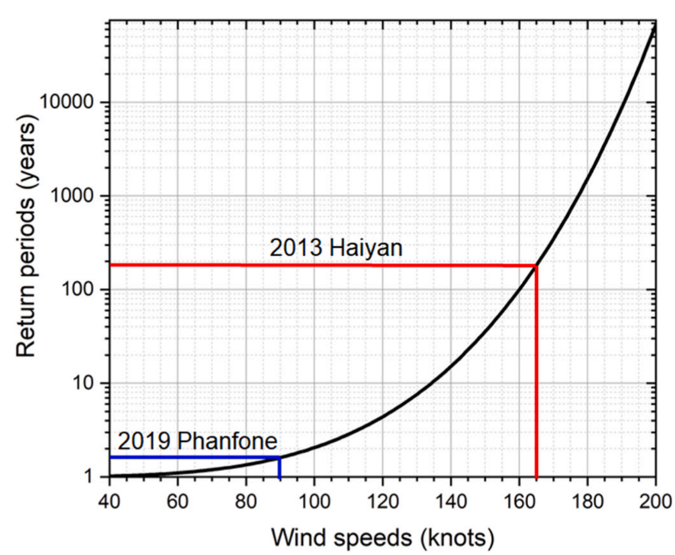

Fig. 7. The relationship between return periods and wind speeds was derived through extreme value analysis using a Weibull distribution. This figure is adapted from Takagi and Esteban (2016).

mangroves were still in an early stage of growth with relatively short trunks.

It is also noteworthy that the mangrove plantation in Paraiso, as shown in Fig. 9c, has been successful without employing wave-dissipation structures (e.g., wooden and rubble breakwaters) to protect young mangroves—a practice commonly utilized at other plantation sites (Sreeranga et al., 2021; Charoenlerkthawin et al., 2024; Takagi

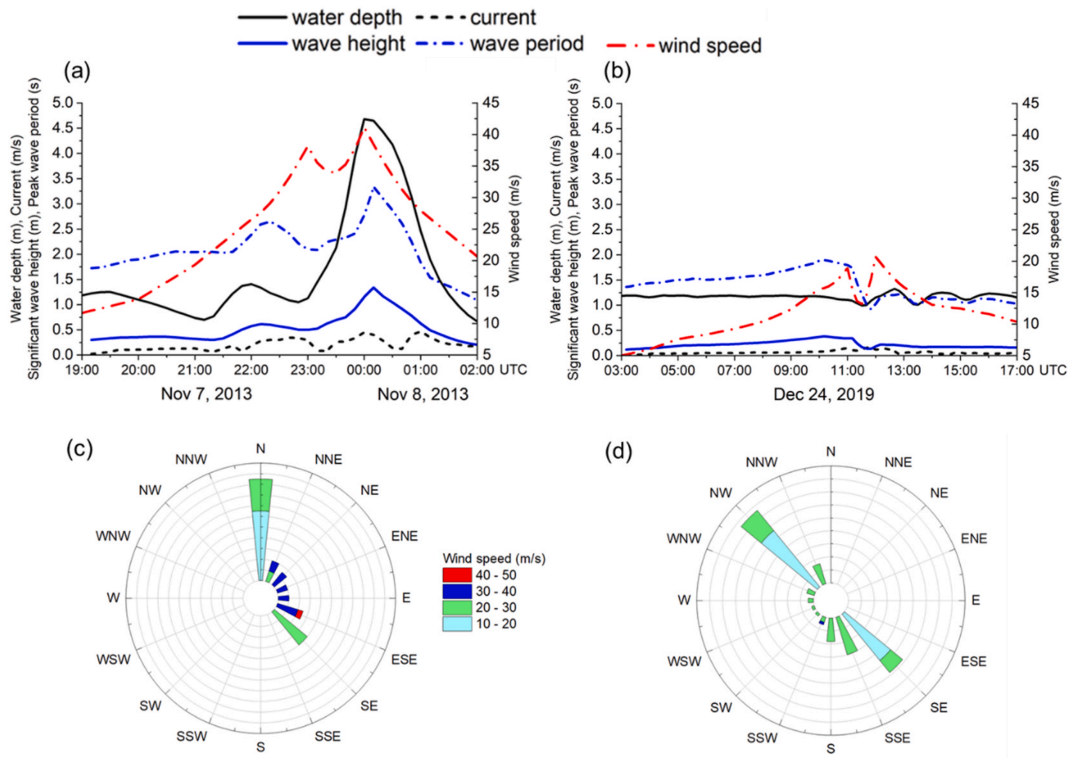

Fig. 8. Estimated water depth and current, wave height and period, and wind speed during the passage of (a) Haiyan and (b) Phanfone; Wind rose charts during the approach of (c) Haiyan and (d) Phanfone. Refer to Fig. 1 for azimuth orientation.

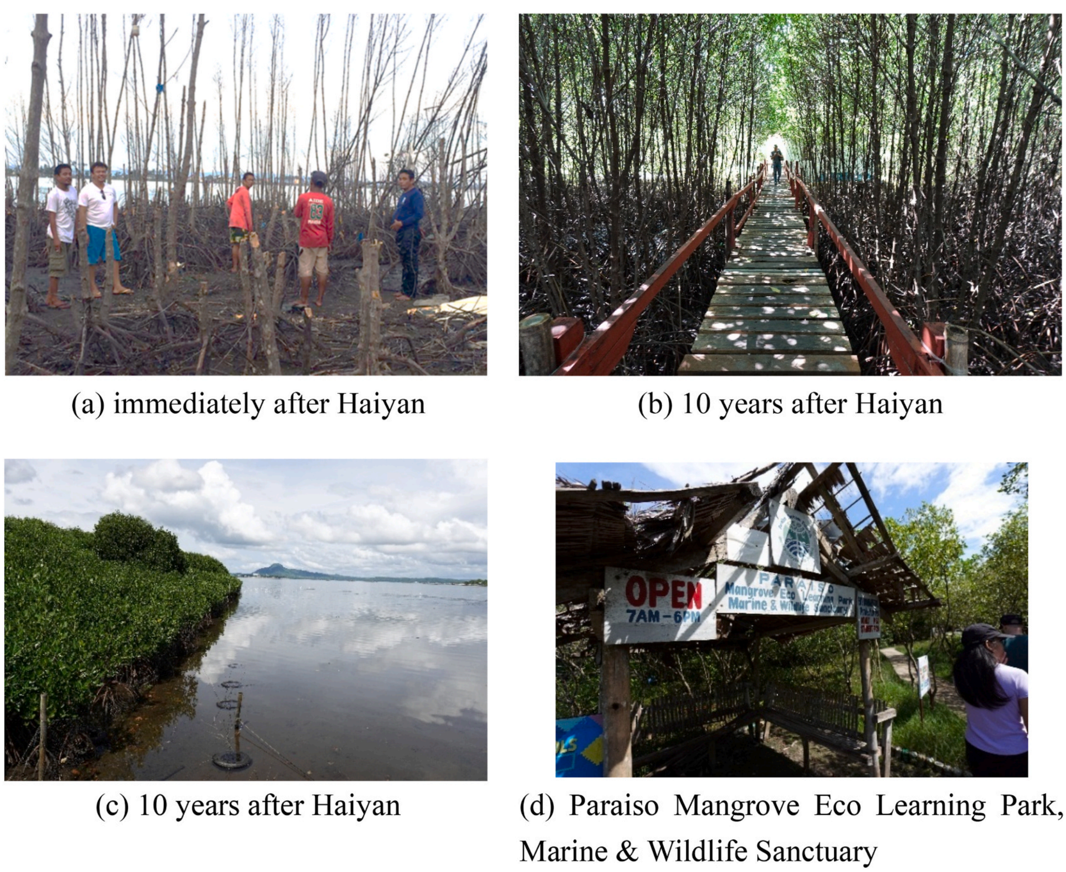

Fig. 9. Visual evidence of significant progress in mangrove reforestation efforts in Paraiso. (a) Photo provided by a local resident. (b)–(d) Photos by the author.

et al., 2025). Such measures have been shown to promote sediment accumulation behind the structures and contribute to creating a more suitable environment for the expansion of the planted mangrove area (Charoenlerkthawin et al., 2024). The Paraiso mangrove has successfully expanded even in the absence of wave-dissipation countermeasures, suggesting that sufficient sediment has naturally accumulated since Typhoon Haiyan, despite the storm's potential to cause significant erosion.

As discussed in the previous section, although Typhoon Phanfone struck Tacloban in 2019, the planted mangroves appeared to have withstood the storm with minimal damage. It was estimated that wave heights around the coast of Paraiso had been sufficiently reduced to 0.4 m. Therefore, its successful growth can also be attributed to the calm hydrodynamic conditions of Cancabato Bay, sheltered by a small northward-extending peninsula that effectively blocks high waves from the offshore region (Fig. 1).

Mangroves typically inhabit calm areas within bays or estuaries, as opposed to locations directly exposed to the open ocean. Consequently, such environments are generally regarded as less susceptible to the impacts of coastal hazards (Chatenoux and Peduzzi, 2007). The active initiatives led by the Paraiso community are arguably the most fundamental factor in the successful mangrove reforestation efforts in Tacloban. However, the successful afforestation ten years after Typhoon Haiyan can be attributed not only to the dedicated efforts of the local people but also to the sheltered environment at the back of the bay, where wave energy is sufficiently low.

6. Conclusions

This study illustrates the relationship between storm intensity during two recent typhoons that struck Leyte Island and the survival of mangrove stands. Given the estimated 200-year return period of Typhoon Haiyan in 2013, the devastation of the mangrove forest in Tacloban might be an inevitable occurrence. *Rhizophora apiculata*, a dominant species in Paraiso, Tacloban City, was severely damaged by the combined effects of storm surge (4.7 m), waves (1.3 m), and strong winds (41 m/s). In contrast, the influence of relatively frequent typhoons, such as Typhoon Phanfone in 2019, constitutes a pivotal determinant for the success of mangrove reforestation efforts. Although Phanfone was evidently strong in intensity, the favorable wind direction resulted in relatively low wave heights. While the estimated maximum wave height during Phanfone was merely 40 cm, this could still pose a considerable impact on immature planted mangroves. This observation demonstrates that healthy young mangroves, just a few years after planting, can be sufficiently resilient to storm disturbances with a return period of 1–2 years. Although significant destruction of mangrove forests may be unavoidable during an unprecedented storm event, prompt initiatives can greatly enhance the success of mangrove regeneration by carefully assessing environmental conditions—for example, whether the location is sufficiently calm under normal wave conditions, or whether the species is capable of firmly rooting along the coast within a relatively short period. The NDVI analysis revealed that the mangrove area had expanded by approximately 80 % ten years after Typhoon Haiyan, primarily as a result of intensive planting activities conducted between 2015 and 2018. Consistent with many previous studies, the present study demonstrated that NDVI is a useful indicator for the preliminary assessment of mangrove forest extent. Nevertheless, because NDVI values are subject to seasonal variability, field observations are indispensable for a more precise assessment of the mangrove extent. The findings of this study are especially valuable for guiding successful mangrove reforestation efforts in typhoon-prone regions. The approach applied in this study is expected to be applicable not only to the Philippines but also to other tropical cyclone-prone regions with extensive mangrove forests, including countries in Asia, Oceania, and Caribbean islands.

Funding

This research was supported by JSPS KAKENHI Grant Number 23K04343.

Declaration of competing interest

The authors declare that they have no known competing financial interests or personal relationships that could have appeared to influence the work reported in this paper.

Data availability

Data will be made available on request.

References

Abayon, M.A., 2023. Mangrove conservation and utilization in Tacloban City, Leyte, Philippines, the. Int. J. Biosci. 23 (1), 284–294.
Alongi, D.M., 2008. Mangrove forests: resilience, protection from tsunamis, and responses to global climate change. Estuar. Coast Shelf Sci. 76, 1–13.
Asbridge, E., Lucas, R., Rogers, K., Accad, A., 2018. The extent of mangrove change and potential for recovery following severe Tropical Cyclone Yasi, Hinchinbrook Island, Queensland, Australia. Ecol. Evol. 8 (21), 10416–10434.
Aung, T.T., Mochida, Y., Than, M.M., 2013. Prediction of recovery pathways of cyclone-disturbed mangroves in the mega delta of Myanmar. For. Ecol. Manag. 293, 103–113.
Barbier, E.B., 2006. Natural barriers to natural disasters: replanting mangroves after the tsunami. Front. Ecol. Environ. 4 (3), 124–131.
Barbier, E.B., et al., 2008. Coastal ecosystem-based management with nonlinear ecological functions and values. Science 319, 321–323.
Battjes, J.A., Janssen, J.P.F.M., 1978. Energy loss and set-up due to breaking of random waves. Proceedings of the 16th Coastal Engineering Conference. ASCE, pp. 569–587.
Bhowmik, A., Cabral, P., 2013. Cyclone sidr impacts on the sundarbans floristic diversity. Earth Sci. Res. 2 (2), 62–79.
Bricker, J.D., Takagi, H., Mas, E., Kure, S., Adriano, B., Yi, C., Roeber, V., 2014. Spatial variation of damage due to storm surge and waves during typhoon Haiyan in the Philippines. Journal of Japan Society of Civil Engineers, Ser. B2 (Coastal Engineering) 70 (2), 231–235.
Cañete, et al., 2018. Flora assessment and total carbohydrate analysis on flower nectars of mangrove species in Leyte Gulf, Maqueda Bay, and Matarinao Bay, Philippines: potential ecosystems for apiculture, Phil. J. Nat. Sci. 23, 79–91.
Carlos, C., Delfino, R.J., Juanico, D.E., David, L., Lasco, R., 2015. Vegetation resistance and regeneration potential of Rhizophora, Sonneratia, and Avicennia in the Typhoon Haiyan-affected mangroves in the Philippines: implications on rehabilitation practices. Climate, Disaster and Development Journal 1 (1), 8p.
Charoenlerkthawin, W., Bidorn, K., Burnett, W.C., Sopen, A., Otarawanna, S., Bidorn, B., 2024. Evaluating the effectiveness of mangrove rehabilitation: a novel approach for sustainable coastal management. J. Environ. Manag.doi. https://doi.org/10.1016/j.jenvman.2024.121673.
Chatenoux, B., Peduzzi, P., 2007. Impacts from the 2004 Indian Ocean Tsunami: analysing the potential protecting role of environmental features. Nat. Hazards 40, 289–304.
Chen, B., Xiao, X., Li, X., Pan, L., Doughty, R., et al., 2017. A mangrove forest map of China in 2015: analysis of time series Landsat 7/8 and Sentinel-1A imagery in Google Earth Engine cloud computing platform. ISPRS J. Photogrammetry Remote Sens. 131, 104–120.
Cho, H., 2017. Toward reforestation to protect from tsunami caused by Typhoon. Japanese Journal of International Forest and Forestry 100.
Dahdouh-Guebas, F., Jayatissa, L.P., Di, Nitto D., Bosire, J.O., Lo, Seen D., Koedam, N., 2005. How effective were mangroves as a defence against the recent tsunami? Curr. Biol. 15 (12), 443–448.
Deltares, 2011. Delft3D-FLOW – Simulation of multi-dimensional Hydrodynamic Flows and Transport Phenomena, Including Sediments, vol. 690p. User Manual Delft3D-FLOW.
Environmental Justice Foundation. Mangroves, 2006. Nature's Defence Against Tsunamis—A Report on the Impact of Mangrove Loss and Shrimp Farm Development on Coastal Defences. Environmental Justice Foundation, London, UK.
FAO: The World's Mangroves 2000-2020, 2023. Food and Agriculture Organization of the United Nations. https://reliefweb.int/report/world/worlds-mangroves-2000-2020. (Accessed 15 June 2025).
Halder, N.K., Merchant, A., Misbahuzzaman, K., Wagner, S., Mukul, S.A., 2021. Why some trees are more vulnerable during catastrophic cyclone events in the Sundarbans mangrove forest of Bangladesh? For. Ecol. Manag. 490, 11.
Headquarters for Earthquake Research Promotion, 2017. Tsunami Prediction Method for Earthquakes with Characterized Source Faults (Tsunami Recipe), 38 pages.
Iuchi, K., 2024. Adaptability of low-income communities in postdisaster relocation: a long-term study following Typhoon Haiyan. J. Am. Plann. Assoc. 90, 2–17.
Kamthonkiat, D., Rodfai, C., Saiwanrungkul, A., Koshimura, S., Matsuoka, M., 2011. Geoinformatics in mangrove monitoring: damage and recovery after the 2004 Indian Ocean tsunami in Phang Nga, Thailand. Nat. Hazards Earth Syst. Sci. 11, 1851–1862.

Kathiresan, K., Rajendran, N., 2005. Coastal mangrove forests mitigated tsunami. Estuar. Coast Shelf Sci. 65, 601–606.
Komen, G.J., Hasselmann, S., Hasselmann, K., 1984. On the existence of a fully developed wind-sea spectrum. J. Phys. Oceanogr. 14 (8), 1271–1285.
Lin, I.I., Pun, I.F., Lien, C.C., 2014. Category-6" supertyphoon Haiyan in global warming hiatus: contribution from subsurface ocean warming. Geophys. Res. Lett.doi. https://doi.org/10.1002/2014GL061281.
Long, J., Giri, C., Primavera, J., Trivedi, M., 2016. Damage and recovery assessment of the Philippines' mangroves following super typhoon Haiyan. Mar. Pollut. Bull. 109, 734–743.
Mikami, T., Shibayama, T., Takagi, H., Matsumaru, R., Esteban, M., Thao, N.D., de Leon, M., Valenzuela, V.P., Oyama, T., Nakamura, R., Kumagai, K., Li, S., 2016. Storm surge heights and damage caused by the 2013 typhoon Haiyan along the Leyte Gulf Coast. Coast. Eng. J. 27p.
Mitsuta, Y., Suenobu, T., Fujii, T., 1988. Supergradient surface wind in the eye of a typhoon. J. Meteorol. Soc. Jpn. 66 (3), 505–508.
MOFA, 2022. Project for resilient community protected by forest restoration from super typhoon "Haiyan". https://www.mofa.go.jp/mofaj/gaiko/oda/region/e_asia/philippines/page22_001577.html. (Accessed 15 June 2025).
Myers, V.A., 1954. Characteristics of United States Hurricanes Pertinent to Levee Design for Lake Okeechobee, vol. 32. Hydrometeorological Report, US Weather Bureau, Florida, p. 106.
Onrizal, Mansor M., 2016. Status of coastal forests of the Northern Sumatra in 2005 (after 2004's tsunami catastrophe). Biodiversitas 17 (1), 44–54.
Patindol, T.A., Casas, J.E.V., 2019. Species diversity and composition of mangroves in Tacloban City, Philippines. Ann. Trop. Res. 41 (2), 67–75.
Primavera, J.H., Esteban, J.M.A., 2008. A review of mangrove rehabilitation in the Philippines: successes, failures and future prospects. Wetlands Ecol Manage 16, 345–358.
Ruan, L., Yan, M., Zhang, L., Fan, X.S., Yang, H., 2022. Spatial-temporal NDVI pattern of global mangroves: a growing trend during 2000–2018. Sci. Total Environ. 844.
Santiago, R.B., Cabahug, Jr.D.M., Alonzo-Pasicolan, S.N., 1990. Identification and Inventory of Philippine forested-wetland Resource, 33/34. Forest Eclogy and Management, pp. 21–44.
Schiermeier, Q., 2013. Did climate change cause Typhoon Haiyan. Nature.
Schloemer, R.W., 1954. Analysis and synthesis of hurricane wind patterns over Lake Okeechobee, Florida. Hydrometerorological Report No. 31.
Spalding, M., Kainuma, M., Collins, L., 2010. World Atlas of Mangroves, ITTO, ISME, FAO. UNESCO-MAB and UNU-INWEH, p. 319.
Sreeranga, S., Takagi, H., Shirai, R., 2021. Community-based portable reefs to promote mangrove vegetation growth: bridging between ecological and engineering principles. Int. J. Environ. Res. Publ. Health 18, 590.
Tajima, et al., 2014. Initial report of JSCE-PICE joint survey on the storm surge disaster caused by typhoon Haiyan. Coast. Eng. J. 56 (1), 12.
Takagi, H., 2018. Long-term design of mangrove landfills as an effective tide attenuator under relative sea-level rise. Sustainability 10, 1045.
Takagi, H., Esteban, M., 2016. Statistics of tropical cyclone landfalls in the Philippines -Unusual characteristics of 2013 typhoon Haiyan. Nat. Hazards 80 (1), 211–222.
Takagi H. Survival of young planted mangroves in a calm bay environment during a tropical cyclone, *Nature-Based Solutions*, Elsevier, vol 4, 2023.
Takagi, H., Heidarzadeh, M., 2023. Coastal disasters in Asia: forecasting, uncovering, Recovering, and mitigation. Coast. Eng. J. 65 (1).
Takagi, H., Esteban, M., Shibayama, T., Mikami, T., Matsumaru, R., Leon, M.D., Thao, N. D., Oyama, T., Nakamura, R., 2014. Track analysis, simulation, and field survey of the 2013 Typhoon Haiyan storm surge. J. Flood Risk Management 10 (1), 42–52.
Takagi, H., Li, S., de Leon, M., Esteban, M., Mikami, T., Matsumaru, R., Shibayama, T., Nakamura, R., 2016. Storm surge and evacuation in urban areas during the peak of a storm. Coast. Eng. 108, 1–9.
Takagi, H., Tomiyasu, R., Oyake, T., Araki, T., Mori, K., Matsubara, Y., Ninomiya, Y., Takata, Y., 2020. Tsunami intrusion through port breakwaters enclosed with self-elevating seawalls. Ocean Engineering, Elsevier 199, 13.
Takagi, H., Prattoyee, F.T., Mitsui, J., Kubota, S., 2025. Design of portable reefs to protect young mangroves. J. Mar. Sci. Eng. 13 (4).
Teh, S.Y., Koh, H.L., Liu, P.L., Ismail, A.I., Lee, H.L., 2009. Analytical and numerical simulation of tsunami mitigation by mangroves in Penang, Malaysia. J. Asian Earth Sci. 36 (1), 38–46.
The Guardian, 2019. Typhoon Phanfone: at least 28 killed in Philippines after Christmas storm. https://www.theguardian.com/world/2019/dec/26/typhoon-phanfone-killed-in-christmas-day-storm. (Accessed 15 June 2025).
Thwin, H.N., Takagi, H., Islam, M.R., 2025. Impact Assessment of 2023 Cyclone Mocha on Vegetation and Flood Using Remote Sensing Image Analysis. Japanese Journal of JSCE.
TIME: The typhoon's toll, 2013. About Time Mag. 182 (22).
Tucker, C.J., 1979. Red and photographic infrared linear combinations for monitoring vegetation. Remote Sens. Environ. 8, 127–150.
Walters, B.B., 2004. Local management of mangrove forests in the Philippines: successful conservation or efficient resource exploitation? Hum. Ecol. 32, 177–195.
Wilchcombe, J., Nishi, R., Simmons, J., Widlansky, M., Tsurunari, Y., 2021. Field survey on storm surge by catastrophic Hurricane Dorian in The Bahamas 2019. Journal of Japan Society of Civil Engineers, Ser. B3 (Ocean Engineering) 77 (2), 289–294.
Win, S. Towprayoon S., Chidthisong, A., 2020. Mangrove status, its ecosystem, and climate change in Myanmar: a study in Ayeyarwaddy Delta Coastal Zone. IOP Conf. Series: Earth and Environmental Science 496, 012007.
Wodehouse, D.C.J., Rayment, M.B., 2019. Mangrove area and propagule number planting targets produce sub-optimal rehabilitation and afforestation outcomes, Estuarine. Coastal and Shelf Science 222, 91–102.
Yang Ju, Iryna Dronova, Qin Ma, Jian Lin, Mika R. Moran, Nelson Gouveia, Hong Hu, Haiwei Yin, Huiyan Shang, Assessing Normalized Difference Vegetation Index as a proxy of urban greenspace exposure, Urban Forestry & Urban Greening, Volume 99, 2024, 128454, ISSN 1618-8667, https://doi.org/10.1016/j.ufug.2024.128454.
Yanagisawa, H., Koshimura, S., Goto, K., Miyagi, T., Imamura, F., Ruangrassamee, A., Tanavud, C., 2009. The reduction effects of mangrove forest on a tsunami based on field surveys at Pakarang Cape, Thailand and numerical analysis, Estuarine. Coastal and Shelf Science 81 (1), 27–37.
Yanagisawa, H., Koshimura, S., Miyagi, T., Imamura, F., 2010. Tsunami damage reduction performance of a mangrove forest in Banda Aceh, Indonesia inferred from field data and a numerical model. Journal of Geophysical Research Oceans 115 (C6).
Zhang, X., Lin, P., Chen, X., 2022. Coastal protection by planted mangrove forest during typhoon Mangkhut. J. Mar. Sci. Eng. 10 (9), 1288.